

# The Higgs mass and CP violation in supersymmetry

Müge Boz

Physics Department, Hacettepe University, 06532, Beytepe, Ankara

## Abstract

In the framework of the minimal SUSY model with explicit CP violation, the one-loop effective potential is computed. It is found that the lightest Higgs mass is quite sensitive to the SUSY CP-phases. Those portions of the parameter space that would be excluded by the recent experimental results become admissible for finite SUSY phases. The CP-odd composition of the lightest Higgs is also analyzed and it is found that it remains less than a per cent unless the  $\mu$  parameter remain below  $2.M_W$ . Due to its restricted parameter space, we work in the Gluino Axion Model; however, the results are of general validity. PACS: 12.60.Jv, 11.30.Er, 12.60.Fr

# 1 Introduction

Presently, the phenomenon of CP nonconservation is one of the key problems from both theoretical and experimental points of views. The observed CP violation in neutral kaon system [1] as well as the electric dipole moment (EDM) of the neutron [2] severely constrain the sources and strength of CP violation in the underlying model. In the standard model (SM) both strong and electroweak interactions violate the CP invariance. It is a well-known fact that the  $\theta$  vacuum [3] violates the CP invariance, and results in a neutron EDM exceeding the present bounds by nine orders of magnitude [4]. This is the source of the strong CP problem – a CP hierarchy and naturalness problem.

In the supersymmetric (SUSY) extensions of the standard electroweak theory (SM) this hierarchy problem still persists. Moreover, there appear novel sources of CP violation coming from the soft supersymmetry breaking mass terms. Though the phases of the soft terms have been shown to relax to CP-conserving points in the minimal model (MSSM) [5], this is not necessarily true in the non-minimal model (NMSSM) [6] containing a singlet. These soft terms contribute to known CP-violating observables [7] (EDM's and neutral meson mixings); however, they also induce CP violation in the Higgs sector as already noted in [8, 9] and [10, 11].

In addition to these CP hierarchy problems, in minimal SUSY model there is another hierarchy problem concerning the Higgsino Dirac mass parameter ( $\mu$ ), that is, this mass parameter follows from the superpotential of the model and there is no telling of at what scale (ranging from  $M_W$  to  $M_{Pl}$ ) it is stabilized.

In Ref. [12] the two hierarchy problems, i.e, the strong CP problem and the  $\mu$  problem are solved in the context of supersymmetry with a new kind of axion [13, 14] which couples to the gluino rather than to quarks. In this model, the invariance of the supersymmetric Lagrangian and all supersymmetry breaking terms under  $U(1)_R$  is guaranteed by promoting the ordinary  $\mu$  parameter to a composite operator involving the gauge singlet  $\hat{S}$  with unit  $R$  charge. When the scalar component of the singlet develops vacuum expectation value (VEV) around the Peccei–Quinn scale  $\sim 10^{11} \text{ GeV}$  an effective  $\mu$  parameter  $\mu \sim \text{a TeV}$  is induced. Besides the low energy theory is identical to minimal SUSY model with all sources of soft SUSY phases. Due to

all these abilities of the model of [12] in solving the hierarchy problems, in the analysis below we will adopt its parameter space. However, as will be commented at the end, the results will have general validity noted earlier in [8, 9].

In this work, our basic goal is to compute the radiatively corrected Higgs masses and mixings taking into account the CP violation effects. It will be seen that the SUSY phases significantly affect the Higgs masses and mixings thereby giving new regions in the parameter space (otherwise excluded) meeting the recent LEP constraints [15]. We will base our calculation to those of [9] by modifying the results appropriately in connection with the Gluino Axion Model of [12]. The main difference with the previous work [8, 9] springs from the fact that all the soft mass parameters in this theory are fixed in terms of the  $\mu$  parameter.

This work is organized as follows. In Sec. II, we compute the mass matrix elements of the Higgs Scalars using the gluino-axion model[12]. In Sec. III, we make the numerical analysis for evaluating the mass of the lightest Higgs boson and analyzing the relative strengts of CP-violating and CP-conserving mixings. In Sec. IV, we conclude the work.

## 2 Higgs Sector in the Gluino-Axion Model

In the gluino-axion model [12] the soft terms of the low energy Lagrangian is identical to those in the general MSSM <sup>1</sup>

$$\begin{aligned}\mathcal{L}_{MSSM}^{soft} = & \tilde{Q}^\dagger M_Q^2 \tilde{Q} + \tilde{u}^{c\dagger} M_{u^c}^2 \tilde{u}^c + \tilde{d}^{c\dagger} M_{d^c}^2 \tilde{d}^c + \tilde{L}^\dagger M_L^2 \tilde{L} + \tilde{e}^{c\dagger} M_{e^c}^2 \tilde{e}^c \\ & + \left\{ A_u \tilde{Q} \cdot H_u \tilde{u}^c + A_d \tilde{Q} \cdot H_d \tilde{d}^c + A_e \tilde{L} \cdot H_d \tilde{e}^c \right\} + h.c. \\ & + M_{H_u}^2 |H_u|^2 + M_{H_d}^2 |H_d|^2 + (\mu B H_u \cdot H_d + h.c.) \\ & + \left\{ M_3 \tilde{\lambda}_3^a \tilde{\lambda}_3^a + M_2 \tilde{\lambda}_2^i \tilde{\lambda}_2^i + M_1 \tilde{\lambda}_1 \tilde{\lambda}_1 + h.c. \right\},\end{aligned}\tag{1}$$

except for the fact that the soft masses are all expressed in terms of the  $\mu$  parameter through appropriate flavour matrices. The flavour matrices form the sources of CP violation and intergenerational mixings in the squark sector. The phases of the trilinear couplings ( $A_{u,d,e}$ ), the gaugino masses

---

<sup>1</sup>Here and in what follows we will neglect the effects of axion, axino, and saxino as their couplings are severely suppressed [12].

$(M_{3,2,1})$ , and the effective  $\mu$ -parameter

$$\mu \equiv v_s^2/M_{Pl} \times e^{-i\theta_{QCD}/3} \sim \text{a TeV} \times e^{-i\theta_{QCD}/3} \quad (2)$$

are the only phases which can generate CP violation observables. In this formula for  $\mu$  parameter  $v_s \sim 10^{11}$  GeV is the Peccei–Quinn scale, and  $\theta_{QCD}$  is the effective QCD vacuum angle. It is known that the dominant corrections are given by the top quark and top squark loops so that we will not need the full flavour structures in [12], instead we will need to specify only the top squark sector:

(i) The top squark soft masses:

$$M_Q^2 = k_Q^2 |\mu|^2, \quad M_{\tilde{u}}^2 = k_u^2 |\mu|^2, \quad M_{\tilde{d}}^2 = k_d^2 |\mu|^2 \quad (3)$$

where  $k_{Q,u,d}$  are real parameters.

(ii) The top squark trilinear coupling

$$A_t = \mu^* k_t, \quad (4)$$

where  $k_t$  is a complex parameter.

Other than these soft masses, it is necessary to know the tree level Higgs soft masses

$$M_{H_u}^2 = y_u |\mu|^2, \quad M_{H_d}^2 = y_d |\mu|^2, \quad \mu B = |\mu_{eff}|^2 \left( \frac{8m_s^2}{v_s^2} + k_\mu \right), \quad (5)$$

where  $m_s^2 \sim v_s^2$  as discussed in [12]. Here  $y_u$  and  $y_d$  are real parameters, and  $k_\mu$  is a complex parameter determining the phase of the  $B$  parameter. As was analyzed in [9] in detail this phase can be identified with the relative phase of the Higgs doublets; hence, there is no CP violation in Higgs sector of (1) at tree level.

After electroweak breaking the Higgs doublets in (1) can be expanded as

$$\begin{aligned} H_d &= \begin{pmatrix} H_d^0 \\ H_d^- \end{pmatrix} = \frac{1}{\sqrt{2}} \begin{pmatrix} v_d + \phi_1 + i\varphi_1 \\ H_d^- \end{pmatrix}, \\ H_u &= \begin{pmatrix} H_u^+ \\ H_u^0 \end{pmatrix} = \frac{e^{i\theta}}{\sqrt{2}} \begin{pmatrix} H_u^+ \\ v_u + \phi_2 + i\varphi_2 \end{pmatrix}. \end{aligned} \quad (6)$$

where  $\tan \beta \equiv v_u/v_d$  as usual, and the angle parameter  $\theta$  is the misalignment between the two Higgs doublets. As in [9] the angle  $\theta$  gets embedded into

the total CP violation angle  $\text{Arg}[\mu A_t]$ , and we will not elaborate radiative corrections to it [16].

As usual, we calculate the Higgs masses and their mixings up to one loop accuracy via

$$M^2 = \left( \frac{\partial^2 V}{\partial \chi_i \partial \chi_j} \right)_0, \text{ where } \chi_i \in \mathcal{B} = \{\phi_1, \phi_2, \varphi_1, \varphi_2\}. \quad (7)$$

where  $V \equiv V_0 + V_{1-loop}$  is the radiatively corrected Higgs potential [9]. As mentioned before we take into account only top quark and top squark loop corrections, which are the dominant ones as long as  $\tan \beta \lesssim 60$ . The radiative corrections depend on the stop mass-squared eigenvalues  $m_{t_{1,2}}^2$

$$m_{t_{1,2}}^2 = \frac{1}{2} \left( (k_u^2 + k_Q^2) |\mu|^2 + 2m_t^2 \mp \Delta_t^2 \right), \quad (8)$$

whose splitting

$$\Delta_t^2 = |\mu| \sqrt{(k_u^2 - k_Q^2)^2 |\mu|^2 + 4m_t^2 (|k_t|^2 + \cot^2 \beta - 2|k_t| \cot \beta \cos \varphi_{kt})}. \quad (9)$$

will play a key rôle in analyzing the results as it depends explicitly on the total CP violation angle

$$\varphi_{kt} = \text{Arg}[\mu A_t] = \text{Arg}[k_t] \quad (10)$$

where  $k_t$  has been defined in (4). One here notices that  $\Delta_t^2$  increases as  $\varphi_{kt}$  changes from 0 to  $\pi$ . This particularly means that the strength of the radiative corrections are modified as  $\varphi_{kt}$  ranges from one CP-conserving point to the next.

We express the Higgs mass-squared matrix

$$M^2 = \begin{pmatrix} M_{11} & M_{12} & M_{13} \\ M_{12} & M_{22} & M_{23} \\ M_{13} & M_{23} & M_{33} \end{pmatrix}, \quad (11)$$

in the basis  $\mathcal{B} = \{\phi_1, \phi_2, \sin \beta \varphi_1 + \cos \beta \varphi_2\}$  using (6). The elements of the mass matrix read as below:

$$M_{11} = M_Z^2 \cos^2 \beta + \tilde{M}_A^2 \sin^2 \beta + \Delta_{11}, \quad (12)$$

$$M_{12} = -(M_Z^2 + \tilde{M}_A^2) \sin \beta \cos \beta + \Delta_{12}, \quad (13)$$

$$M_{22} = M_Z^2 \sin^2 \beta + \tilde{M}_A^2 \cos^2 \beta + \Delta_{22}, \quad (14)$$

$$M_{13} = r\Delta, \quad (15)$$

$$M_{23} = s\Delta, \text{ and }, \quad (16)$$

$$M_{33} = \tilde{M}_A^2 + \Delta, \quad (17)$$

where the radiative corrections are generically denoted by  $\Delta_{ij}$ .  $\Delta_{11,12,22}$  do also exit in the CP conserving limit (See the references in [9].); however, the quantity  $\Delta$  (to which  $M_{13}$  and  $M_{23}$  are proportional) is genuinely generated by the SUSY CP-violation effects. These correction terms have the expressions:

$$\Delta_{11} = -2\beta_{ht} \frac{|\mu|^4 m_t^2 (|k_t| \cos \varphi_{kt} - \cot \beta)^2}{\Delta_{\tilde{t}}^4} g(m_{\tilde{t}_1}^2, m_{\tilde{t}_2}^2) , \quad (18)$$

$$\begin{aligned} \Delta_{12} = & -2\beta_{ht} m_t^2 |\mu|^2 \left\{ \frac{|k_t| \cos \varphi_{kt} - \cot \beta}{\Delta_{\tilde{t}}^2} \log \frac{m_{\tilde{t}_2}^2}{m_{\tilde{t}_1}^2} \right. \\ & - |\mu|^2 |k_t| \frac{(|k_t| \cos \varphi_{kt} - \cot \beta)^2 + |k_t| (|k_t| - \cot \beta) \sin^2 \varphi_{kt}}{\Delta_{\tilde{t}}^4} \\ & \left. \times g(m_{\tilde{t}_1}^2, m_{\tilde{t}_2}^2) \right\} , \end{aligned} \quad (19)$$

$$\begin{aligned} \Delta_{22} = & 2\beta_{ht} m_t^2 \left\{ \log \frac{m_{\tilde{t}_2}^2 m_{\tilde{t}_1}^2}{m_t^4} + \frac{2|k_t| |\mu|^2 (|k_t| - \cot \beta \cos \varphi_{kt})}{\Delta_{\tilde{t}}^2} \right. \\ & \left. \times \log \frac{m_{\tilde{t}_2}^2}{m_{\tilde{t}_1}^2} - \frac{|k_t|^2 |\mu|^4 (|k_t| - \cot \beta \cos \varphi_{kt})^2}{\Delta_{\tilde{t}}^4} g(m_{\tilde{t}_1}^2, m_{\tilde{t}_2}^2) \right\} \end{aligned} \quad (20)$$

and finally ,

$$\Delta = -2\beta_{ht} m_t^2 \frac{\sin^2 \varphi_{kt}}{\sin^2 \beta} \frac{|\mu|^4 |k_t|^2}{\Delta_{\tilde{t}}^4} g(m_{\tilde{t}_1}^2, m_{\tilde{t}_2}^2) , \quad (21)$$

where  $\beta_{ht} = 3h_t^2/16\pi^2$ , and the adimensional parameters  $r$  and  $s$  are given by

$$r = \frac{\sin \beta}{\sin \varphi_{kt}} \frac{|k_t| \cos \varphi_{kt} - \cot \beta}{|k_t|} , \text{ and} \quad (22)$$

$$\begin{aligned} s = & \frac{\sin \beta}{\sin \varphi_{kt}} \{ (|k_t| - \cot \beta \cos \varphi_{kt}) \\ & - \frac{1}{|k_t| |\mu|^2 g(m_{\tilde{t}_1}^2, m_{\tilde{t}_2}^2)} \Delta_{\tilde{t}}^2 \log \frac{m_{\tilde{t}_2}^2}{m_{\tilde{t}_1}^2} \} . \end{aligned} \quad (23)$$

In the above formulae  $g(x, y)$  is the scale-independent loop function defined by

$$g(x, y) = -2 + \frac{y+x}{y-x} \log \frac{y}{x} . \quad (24)$$

We diagonalize the Higgs mass-squared matrix (11) by the similarity transformation

$$\mathcal{R} M^2 \mathcal{R}^T = \text{diag}(m_{h_1}^2, m_{h_1}^2, m_{h_1}^2) \quad (25)$$

where  $\mathcal{R}\mathcal{R}^T = 1$ . One of the most important quantities is the percentage CP composition of a given mass-eigenstate Higgs boson. Letting  $H_1$  be the lightest of all three its CP composition in terms of the basis elements is defined by

$$\rho_i = 100 \times |\mathcal{R}_{1i}|^2; \quad i = 1, 2, 3. \quad (26)$$

In what follows one of the main concerns will be the CP odd composition,  $\rho_3$ , of the lightest Higgs as it can offer new opportunities at colliders for observing the Higgs boson [8]. Moreover, we will discuss in detail the dependence of the lightest Higgs mass on the CP-breaking angle in reference to previous theoretical [8, 9] as well as the recent experimental bounds [15].

### 3 Numerical Analysis

Using the formulae in the last section we will now analyze several quantities in a wide range of the parameter space. Since the  $\mu$  parameter is already stabilized to the weak scale, as a consequence of the naturalness, all dimensionless quantities are expected to be  $\mathcal{O}(1)$ . Therefore, as a representative point in the parameter space we take

$$k_Q = k_u = |k_t| = 1, \quad (27)$$

and let  $M_A$  vary from  $|\mu|$  to  $5|\mu|$  for each  $\mu$  value. Moreover, we study two values of  $\tan\beta$ :  $\tan\beta = 4$  and  $\tan\beta = 30$  to illustrate the variation of Higgs masses and mixings.

It is now a well-known fact that the heavy Higgs bosons, which are out of reach of the present colliders, have no definite CP quantum number for most of the MSSM parameter space. Before NLC or TESLA operates, it will be hard to observe them, and thus, we restrict our discussions to the lightest Higgs only. Its CP-odd composition as well as its mass for a given portion of the parameter space are of prime importance in the light of present LEP experiments [15].

Fig. 1 and Fig. 2 illustrate the dependence of the lightest Higgs mass on  $\varphi_{kt}$  for  $\tan\beta = 4$  and  $\tan\beta = 30$ . In each figure  $|\mu|$  changes from  $100 \text{ GeV}$  to  $500 \text{ GeV}$  and simultaneously  $M_A/|\mu|$  varies from 1 to 5. One immediately observes that for all values of the parameters,  $m_h$  increases with  $\varphi_{kt}$  for

$\tan\beta = 4$  (Fig. 1) whereas it remains constant for  $\tan\beta = 30$  (Fig. 2). This saturation effect in the Higgs mass can be easily understood by observing that the radiative corrections depend strongly on the stop splitting  $\Delta_t^2$ . This quantity depends explicitly on  $\varphi_{kt}$  such that

$$\frac{\Delta_t^2(\pi)}{\Delta_t^2(0)} \sim \sqrt{\frac{1 + \sin 2\beta}{1 - \sin 2\beta}}, \quad (28)$$

that is, it increases with increasing  $\varphi_{kt}$ . However, (28) decreases with increasing  $\tan\beta$ . Indeed, it approaches to unity in the large  $\tan\beta$  limit. Therefore, radiative corrections to  $m_h$  which are sensitive to variations in  $\varphi_{kt}$  are suppressed in large  $\tan\beta$  regime. In the light of these observations it is clear that  $m_h$  is much more flat for  $\tan\beta = 30$  (Fig. 2) compared to that for  $\tan\beta = 4$  (Fig. 1).

It is important to discuss  $m_h$  in the light of recent experimental data [15] which require  $m_h \gtrsim 110 \text{ GeV}$ . Imposing this constraint on  $m_h$  one observes that that portion of the parameter space for which  $\tan\beta = 4$  and  $0 \lesssim \varphi_{kt} \lesssim \pi/2$  is already discarded (Fig. 1). However, the remaining half of the total  $\varphi_{kt}$  range  $\pi/2 \lesssim \varphi_{kt} \lesssim \pi$  still satisfies the bound  $m_h \gtrsim 110 \text{ GeV}$ . Numerically, the Higgs mass changes by  $\mathcal{O}(10 \text{ GeV})$  as  $\varphi_{kt}$  ranges from 0 to  $\pi$ . Clearly, this region of the parameter space would have been discarded by the experimental constraint were not it for the  $\varphi_{kt}$  dependence of the Higgs mass. In contrast to  $\tan\beta = 4$  case, for large  $\tan\beta$  the experimental constraint is satisfied for all values of  $\varphi_{kt}$  since  $m_h \gtrsim 110 \text{ GeV}$  for most of the parameter space (Fig. 2). The dependence of the Higgs mass on the CP violation angle has also been noted in [8] for general MSSM with a limited range of the parameters.

In Figs. 3 and 4 we illustrate the  $\varphi_{kt}$  dependence of  $\rho_3$  designating the CP-odd percentage composition of the lightest Higgs. As is seen from Fig. 3, CP-odd component of  $H_1$  never exceeds 0.025% in the entire range of  $\varphi_{kt}$ . Compared to its CP-even compositions (which form the remaining percentage) this CP-odd component is extremely small to cause observable effects. It may, however, be still important when vertex corrections are included [8]. For large  $\tan\beta$  (Fig. 4) the CP-odd content of  $H_1$  relatively increases reaching the maximum value of  $\mathcal{O}(3\%)$  for  $|\mu| \sim 100 \text{ GeV}$  as indicated by Figs. 5 and 6. It is worth noting that it is not possible to increase the CP-odd composition of the lightest Higgs boson to the order of 1% level unless one



chooses the  $\mu$  unrealistically small. In this sense, the lightest Higgs remains practically CP–even for  $|\mu| \gtrsim 2 \cdot M_W$ . Obviously, if it were carrying large enough CP odd composition this would bring about new opportunities for observing the lightest Higgs as LEP or LHC in near future [8, 17].

Depicted in Figs. 5 and 6, are the CP–odd composition ( $\rho_3$ ) of the lightest Higgs as a function of  $|\mu|$  for  $\tan \beta = 4$  and  $\tan \beta = 30$ , respectively. In both cases  $\rho_3$  decreases with  $|\mu|$ . In Fig. 5 it starts  $3 \times 10^{-2}\%$  level and decreases rapidly with  $|\mu|$ , falling far below  $10^{-2}\%$  for  $|\mu| \gtrsim 300 \text{ GeV}$ . In Fig. 6, for the ease of following, we cut the vertical axis at  $\rho_3 = 0.5\%$ ; however, it actually extends to  $\sim 3\%$  at  $|\mu| = 100 \text{ GeV}$ , consistent with Fig. 4. As in Fig. 5 it again decreases with increasing  $|\mu|$  so that (remembering that  $M_A \propto |\mu|$  for the model under concern) unless  $|\mu|$  is chosen small (equivalently unless the Peccei–Quinn scale is pushed down towards the lower limit of the allowed *axion window* [12, 14]) one cannot increase the CP–odd composition of the lightest Higgs boson – the one that can be observed at LEP soon, if any.

## 4 Conclusion

From the analysis of the mass and the CP–odd composition of the lightest Higgs we conclude that

- The lightest Higgs mass is quite sensitive to the SUSY CP phases, thanks to which there arise new regions of the SUSY parameter space in which the present experimental constraints are satisfied,
- The CP–odd content of the lightest Higgs gains an appreciable value only for small values of  $|\mu|$  namely  $|\mu| \lesssim 2 \cdot M_W$ ,
- The Gluino Axion Model, besides solving the strong CP and  $\mu$ –problems in an economical way, provides a quite restricted parameter space due to the naturalness requirements.

## 5 Acknowledgements

The author gratefully acknowledges the hospitality at The Abdus Salam ICTP where part of this work is done. She also thanks D. A. Demir for useful discussions.

## References

- [1] J. H. Christenson, J. W. Cronin, V. L. Fitch and R. Turlay, Phys. Rev. Lett. **13**, 138 (1964); A. Alavi-Harati *et al.* [KTeV Collaboration], Phys. Rev. Lett. **83**, 917 (1999) [hep-ex/9902029].
- [2] P. G. Harris *et al.*, Phys. Rev. Lett. **82**, 904 (1999).
- [3] C. G. Callan, R. F. Dashen and D. J. Gross, Phys. Lett. **B63**, 334 (1976); R. Jackiw and C. Rebbi, Phys. Rev. Lett. **37**, 172 (1976).
- [4] V. Baluni, Phys. Rev. **D19**, 2227 (1979); R. J. Crewther, P. Di Vecchia, G. Veneziano and E. Witten, Phys. Lett. **B88**, 123 (1979).
- [5] S. Dimopoulos and S. Thomas, Nucl. Phys. **B465**, 23 (1996) [hep-ph/9510220].
- [6] D. A. Demir, hep-ph/9911435.
- [7] M. Dugan, B. Grinstein and L. Hall, Nucl. Phys. **B255**, 413 (1985).
- [8] D. A. Demir, Phys. Lett. **B465**, 177 (1999) [hep-ph/9809360]; Nucl. Phys. Proc. Suppl. **81**, 224 (2000) [hep-ph/9907279].
- [9] D. A. Demir, Phys. Rev. **D60**, 055006 (1999) [hep-ph/9901389].
- [10] A. Pilaftsis, Phys. Lett. **B435**, 88 (1998) [hep-ph/9805373]; A. Pilaftsis and C. E. Wagner, Nucl. Phys. **B553**, 3 (1999) [hep-ph/9902371].
- [11] S. Y. Choi, M. Drees and J. S. Lee, Phys. Lett. **B481**, 57 (2000) [hep-ph/0002287];
- [12] D. A. Demir and E. Ma, hep-ph/0004148.
- [13] R. D. Peccei and H. R. Quinn, Phys. Rev. Lett. **38**, 1440 (1977);
- [14] J. E. Kim, Phys. Rev. Lett. **43**, 103 (1979); M. A. Shifman, A. I. Vainshtein and V. I. Zakharov, Nucl. Phys. **B166**, 493 (1980); M. Dine, W. Fischler and M. Srednicki, Phys. Lett. **B104**, 199 (1981).
- [15] A. Read, <http://lephiggs.web.cern.ch/LEPHIGGS/talks/index.html>.

- [16] D. A. Demir, Phys. Rev. **D60**, 095007 (1999) [hep-ph/9905571]; S. Y. Choi, hep-ph/9908397.
- [17] S. Y. Choi and J. S. Lee, Phys. Rev. **D61**, 015003 (2000) [hep-ph/9907496]; Phys. Rev. **D61**, 111702 (2000) [hep-ph/9909315]. Phys. Rev. **D61**, 115002 (2000) [hep-ph/9910557]; Phys. Rev. **D62**, 036005 (2000) [hep-ph/9912330].

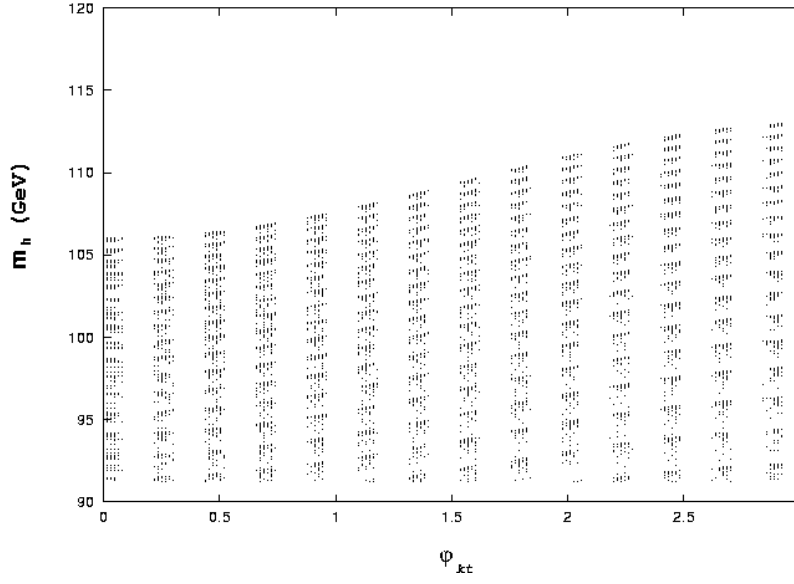


Figure 1: The mass,  $m_h$ , of the lightest Higgs boson as a function of  $\varphi_{kt}$  for  $\tan\beta = 4$ .  $m_h(\phi_{kt} = \pi)$  is larger than  $m_h(\phi_{kt} = 0)$  by  $\sim 10$  GeV due to the enhancements in the radiative corrections as  $\varphi_{kt}$  ranges from 0 to  $\pi$  (see the text).

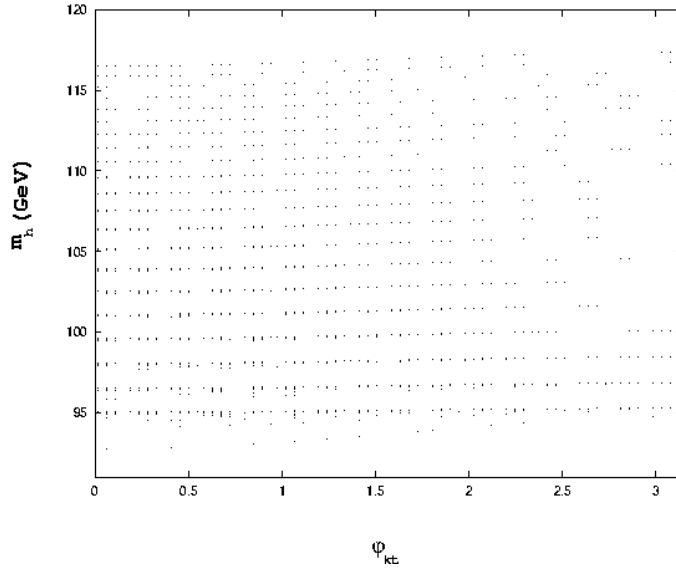


Figure 2: The same as Fig. 1 but for  $\tan\beta = 30$ . Sensitivity of  $m_h$  on  $\phi_{kt}$  is washed out in large  $\tan\beta$  regime (see the text).

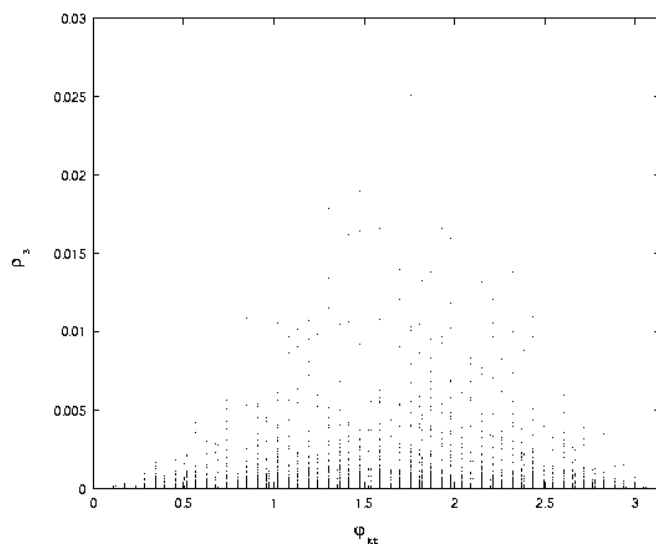


Figure 3: The CP-odd composition ( $\rho_3$ ) of the lightest Higgs as a function of  $\varphi_{kt}$  for  $\tan\beta = 4$ .

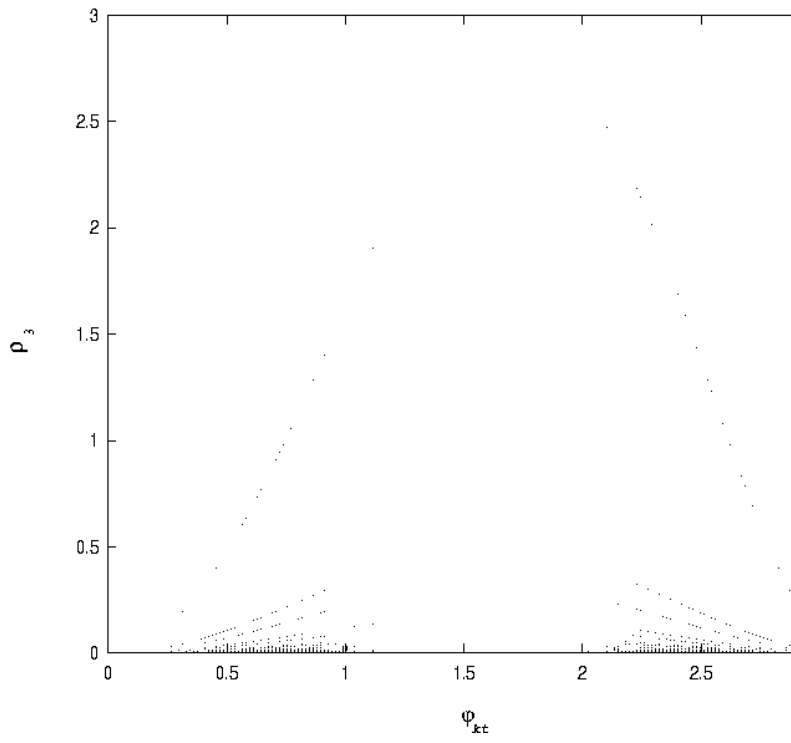


Figure 4: The same as Fig. 3 but for  $\tan \beta = 30$ .

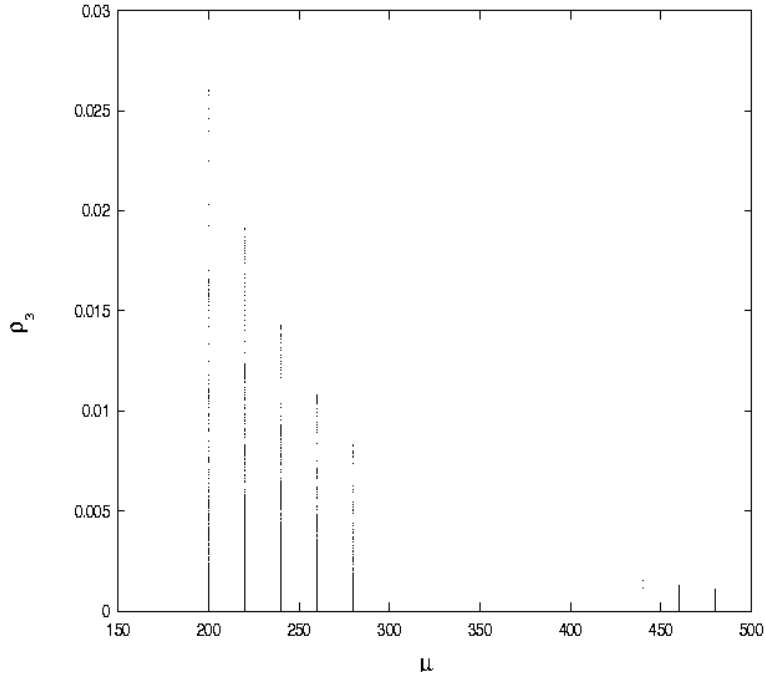


Figure 5: The CP-odd composition ( $\rho_3$ ) of the lightest Higgs as a function of  $|\mu|$  for  $\tan\beta = 4$ .



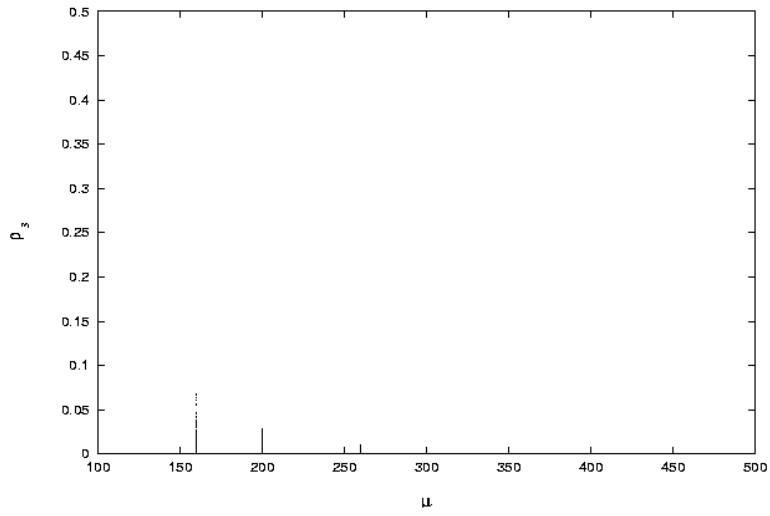


Figure 6: The same as Fig. 5 but for  $\tan\beta = 30$  (Actually, the graph extends to  $\rho_3 \sim 3\%$  at  $|\mu| = 100$  GeV).